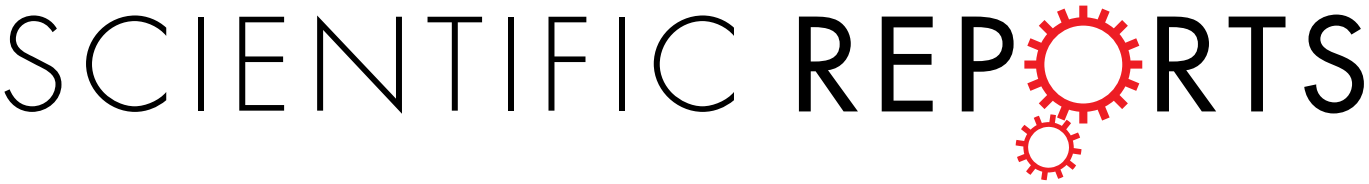

OPEN

Received: 18 August 2017
Accepted: 19 November 2017
Published online: 07 December 2017

Electrically Tunable Fano Resonance from the Coupling between Interband Transition in Monolayer Graphene and Magnetic Dipole in Metamaterials

Bo Liu[1], Chaojun Tang[2], Jing Chen[3,4,5], Mingwei Zhu[5], Mingxu Pei[1] & Xiaoqin Zhu[1]

Fano resonance modulated effectively by external perturbations can find more flexible and important applications in practice. We theoretically study electrically tunable Fano resonance with asymmetric line shape over an extremely narrow frequency range in the reflection spectra of metamaterials. The metamaterials are composed of a metal nanodisk array on graphene, a dielectric spacer, and a metal substrate. The near-field plasmon hybridization between individual metal nanodisks and the metal substrate results into the excitation of a broad magnetic dipole. There exists a narrow interband transition dependent of Fermi energy E_f, which manifests itself as a sharp spectral feature in the effective permittivity ε_g of graphene. The coupling of the narrow interband transition to the broad magnetic dipole leads to the appearance of Fano resonance, which can be electrically tuned by applying a bias voltage to graphene to change E_f. The Fano resonance will shift obviously and its asymmetric line shape will become more pronounced, when E_f is changed for the narrow interband transition to progressively approach the broad magnetic dipole.

Fano resonance in a variety of plasmonic nanostructures and metamaterials has been drawing a lot of attentions in the past decade[1–4], thanks to its great potential for many applications such as refractive-index sensing or biosensing[5–12], surface-enhanced Raman scattering (SERS)[13], light emission enhancement[14,15], nonlinear optical process[16,17], slowing light[18], and so on. In order to obtain Fano resonance, breaking the geometric symmetry has been widely explored for a sharp subradiant (dark) mode to be excited and then interact with a broad superradiant (bright) mode[5–8,19,20], although symmetry breaking is not mandatory for Fano resonance in some nanostructures[21,22]. Recently, there has been increasing interest in dynamically tunable Fano resonance whose resonance wavelength and excitation strength can be changed by internal or external parameters, because tunable Fano resonance can find more flexible and important applications in practice. A very effective approach to tune Fano resonance is directly adjusting the structural parameters of plasmonic nanostructures and metamaterials[23–26]. Fano resonance can also be tuned by external mechanical stress[27], voltages[28], temperature[29], and magnetic field[30]. Furthermore, some studies have demonstrated all-optical tunable Fano resonance by operating light pump intensity[31–33].

Monolayer graphene exhibits intriguing electronic, optical, and mechanical properties, and is promising in optoelectronics, photonics, plasmonics, and metamaterials[34]. Especially, the complex surface conductivity of graphene can be rapidly and dramatically changed by electric gating, which has been utilized for realizing

[1]School of Mathematics and Physics, Jiangsu University of Technology, Changzhou, 213001, China. [2]COOR, Collaborative Innovation Center for Information Technology in Biological and Medical Physics, College of Science, Zhejiang University of Technology, Hangzhou, 310023, China. [3]College of Electronic and Optical Engineering & College of Microelectronics, Nanjing University of Posts and Telecommunications, Nanjing, 210023, China. [4]State Key Laboratory of Millimeter Waves, Southeast University, Nanjing, 210096, China. [5]National Laboratory of Solid State Microstructures and Department of Materials Science and Engineering, Nanjing University, Nanjing, 210093, China. Bo Liu, Chaojun Tang and Jing Chen contributed equally to this work. Correspondence and requests for materials should be addressed to C.T. (email: chaojuntang@126.com) or J.C. (email: jchen@njupt.edu.cn)

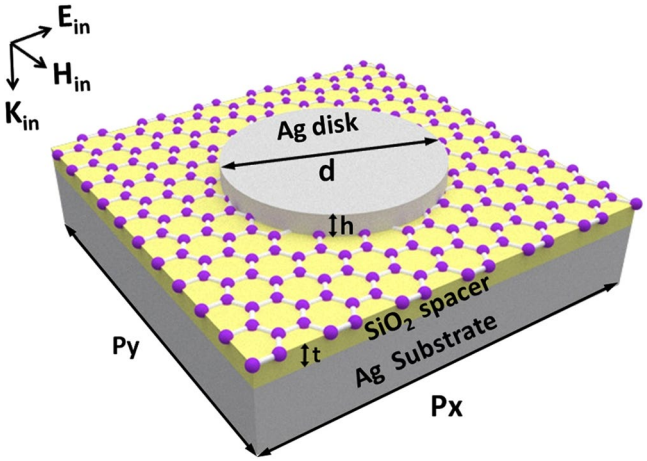

Figure 1. The designed metamaterials for electrically tunable Fano resonance. The period in the x (y) directicon is p_x (p_y). The SiO_2 spacer has a thickness of t. The Ag nanodisk has a diameter of d and a height of h. Light is normally incident, with a polarization along the x direction.

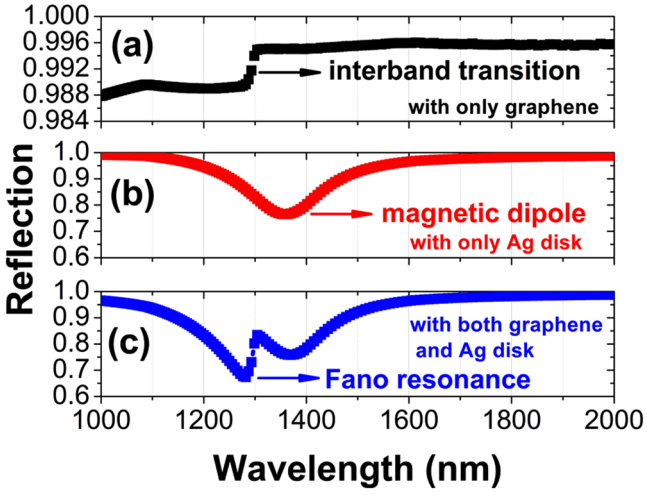

Figure 2. Calculated reflection spectra of metamaterials at normal incidence with only monolayer graphene (**a**), only Ag disk (**b**), and both monolayer graphene and Ag disk (**c**), as schematically shown in Fig. 1. Geometrical and physical parameters: $d = 300$ nm, $h = 50$ nm, $t = 30$ nm, $p_x = p_y = 500$ nm, $E_f = 0.48$ eV, $\tau = 0.50$ ps, $T = 300$ K, $t_g = 0.35$ nm.

electronically tunable Fano resonance in metallic nanostructures and metamaterials with monolayer graphene integrated therein[35–41]. Moreover, very similar to noble metals, graphene in itself is able to support surface plasmon resonances (SPRs) in the mid-infrared and terahertz (THz) regime. Therefore, very recently there also have been many efforts to realize electronically tunable Fano resonance by carefully engineering graphene into nanostructures with various morphologies[42–51].

It is well known that naturally occurring materials exhibit the saturation of the magnetic response beyond the THz regime. In the absence of natural magnetism, most Fano resonances reported so far are mainly based on purely electric effect. However, in the past several years there is also increasing interest in Fano resonance based on magnetic effects in metamaterials[52–59]. But, up to now there are only few researches on electronically tunable Fano resonance by graphene based on magnetic effect[60].

We will theoretically study electrically tunable Fano resonance with asymmetric line shape over an extremely narrow frequency range in the reflection spectra of metamaterials. The metamaterials are composed of a metal nanodisk array on graphene, a dielectric spacer, and a metal substrate. The near-field plasmon hybridization between individual metal nanodisks and the metal substrate results into the excitation of a broad magnetic dipole. There exists a narrow interband transition dependent of Fermi energy E_f, which manifests itself as a sharp spectral feature in the effective permittivity ε_g of graphene. The coupling of the narrow interband transition to the broad magnetic dipole leads to the appearance of Fano resonance, which can be electrically tuned by applying a bias voltage to graphene to change E_f. The Fano resonance will shift obviously and its asymmetric line shape will become more pronounced, when E_f is changed for the narrow interband transition to progressively approach the broad magnetic dipole.

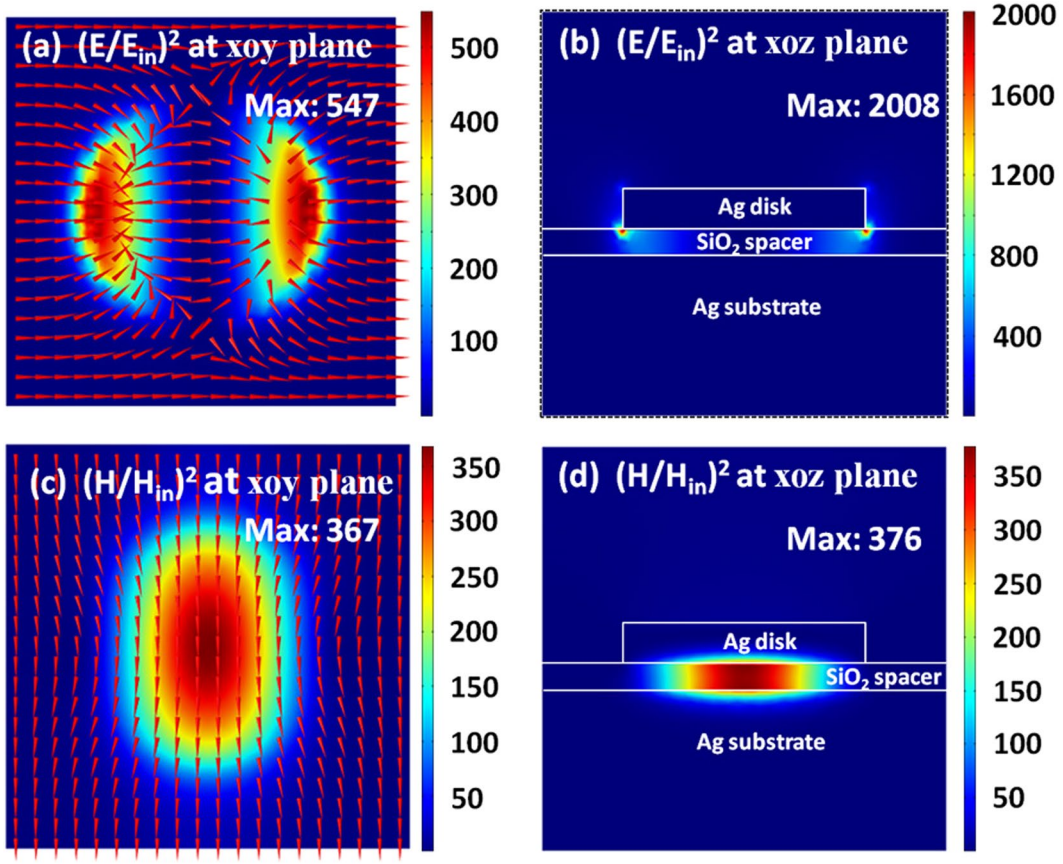

Figure 3. Electromagnetic field distributions on the *xoy* (**a**,**c**) and *xoz* (**b**,**d**) planes, at the resonance wavelength of magnetic dipole. The directions of electromagnetic fields are represented by the red arrows in (**a**,**c**). White lines in (**b**,**d**) outline the boundaries of different regions.

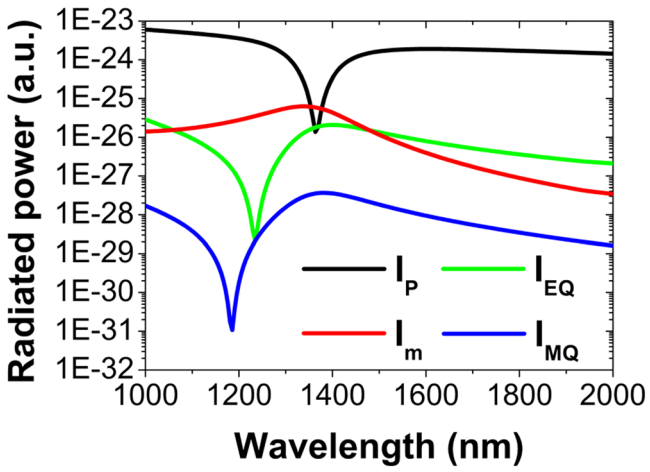

Figure 4. Radiated power from electric dipolar moment I_p, magnetic dipolar moment I_m, electric quadrupole dipolar moment I_{EQ}, and magnetic quadrupole dipolar moment I_{MQ}.

Results

The designed metamaterials for electrically tunable Fano resonance are schematically shown in Fig. 1, which consist of an Ag nanodisk array on a graphene sheet, a SiO_2 spacer, and an Ag substrate. In this work, the reflection and absorption spectra, and the distributions of electromagnetic fields are calculated by "EastFDTD, version 5.0"[61]. The refractive index of SiO_2 is 1.45, and experimental data are used for the permittivity of Ag[62]. Graphene has a complex surface conductivity σ, which is the sum of intraband term σ_{intra} and interband term σ_{inter}[63,64], expressed as follow:

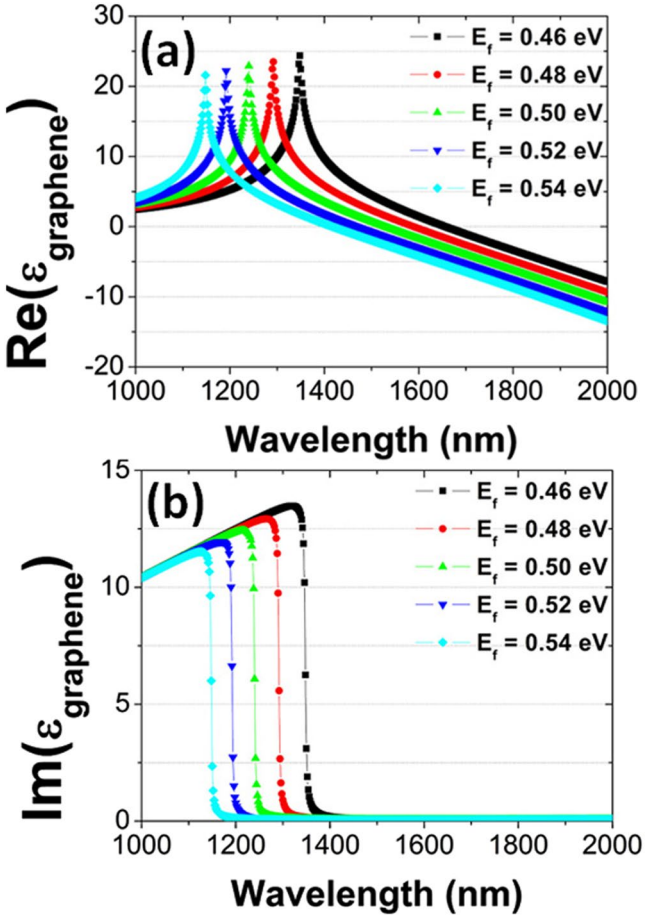

Figure 5. The real (**a**) and imaginary (**b**) parts of the effective permittivity ε_g of graphene as a function of wavelength, with Fermi energy E_f varied from 0.46 to 0.54 eV in steps of 0.2 eV. The other parameters are kept fixed.

$$\sigma_{\text{intra}} = \frac{ie^2 k_B T}{\pi\hbar^2(\omega + i/\tau)}\left(\frac{E_f}{k_B T} + 2\ln(e^{-\frac{E_f}{k_B T}} + 1)\right), \sigma_{\text{inter}} = \frac{ie^2}{4\pi\hbar}\ln\left(\frac{2E_f - (\omega + i/\tau)\hbar}{2E_f + (\omega + i/\tau)\hbar}\right).$$

In the above expression, ω is light frequency, e is electron charge, $\hbar$ is reduced Planck constant, E_f is Fermi energy, τ is relaxation time, k_B is Boltzmann constant, and T is temperature. The effective permittivity ε_g of graphene could be written as $\varepsilon_g = 1 + i\sigma/(\varepsilon_0\omega t_g)$, where ε_0 is vacuum permittivity, and t_g is graphene thickness.

Figure 2(a) presents the reflection spectra in the case of only monolayer graphene at the SiO_2 surface (i.e., the remainder after removing the Ag nanodisk in Fig. 1). In the reflection spectra, one can see an abrupt change around 1300 nm, which results from the narrow interband transition in the monolayer graphene. Figure 2(b) shows the normal-incidence reflection spectra, in the case of only Ag nanodisks at the surface of the SiO_2 spacer supported on the Ag substrate (i.e., the remainder after removing the graphene in Fig. 1). A broad reflection dip centered at 1357 nm is observed, due to the excitation of magnetic dipole from the near-field plasmon hybridization between individual Ag nanodisks and the Ag substrate. Figure 2(c) shows the normal-incidence reflection spectra of metamaterials schematically shown in Fig. 1. In this case, Fano resonance appears and exhibits a pronounced asymmetric line shape with a sharp feature over an extremely narrow wavelength range near 1300 nm in the reflection spectra. The appearance of Fano resonance is from the coupling between the narrow interband transition in graphene and the broad magnetic dipole in metamaterials.

Discussion

To confirm that the broad reflection dip in Fig. 2(b) is because of the excitation of a magnetic dipole in metamaterials, Fig. 3 plots the distributions of electromagnetic fields at the resonance wavelength of 1357 nm. The electric fields have two obvious "hotspots" in the vicinity of the nanodisk (see Fig. 3(a) and (b)), and the magnetic fields have a "hotspot" between the nanodisk and the substrate (see Fig. 3(c) and (d)). Such a field distribution is closely related to the excitation of a magnetic dipole[65–67]. To further demonstrate that the broad reflection dip is closely related to the excitation of a magnetic dipolar mode, we have also calculated the radiated power from electric

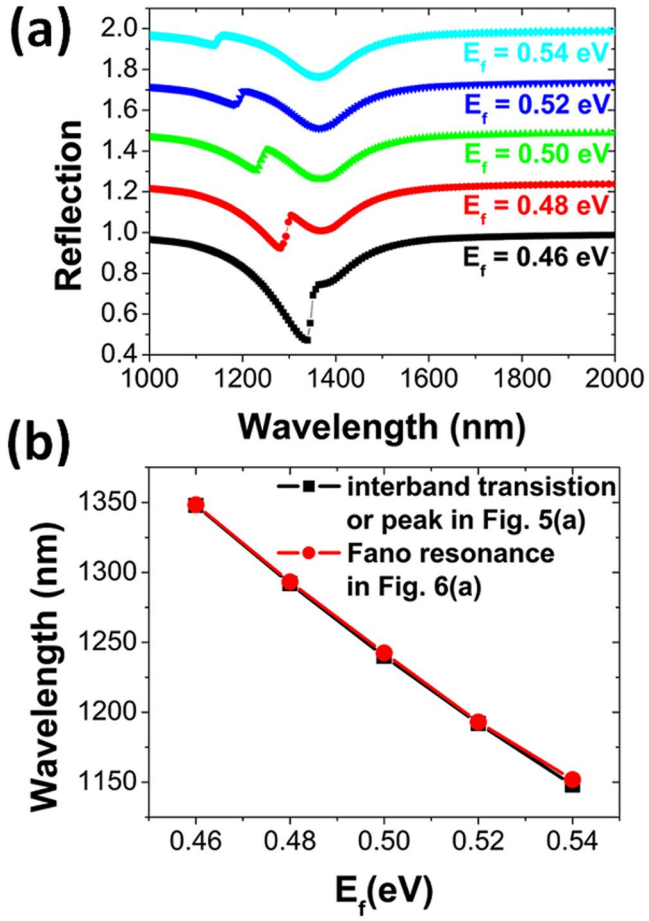

Figure 6. (**a**) Normal-incidence reflection spectra of metamaterials schematically shown in Fig. 1, with Fermi energy E_f varied from 0.46 to 0.54 eV in steps of 0.2 eV. The other parameters are kept fixed. For clarity, individual spectra are vertically offset by 0.25 from one another, respectively. (**b**) The positions of Fano resonance and interband transistion as a function of E_f.

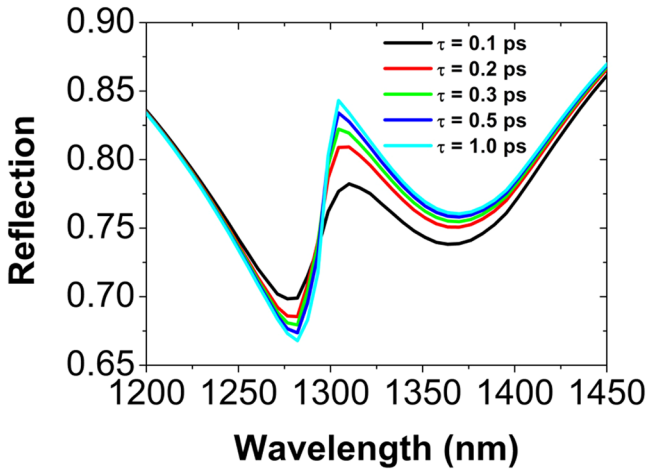

Figure 7. Normal-incidence reflection spectra of metamaterials schematically shown in Fig. 1, with the relaxation time of electron-phonon $\tau = 0.1$, 0.2, 0.3, 0.5, and 1.0 ps. The other parameters are kept fixed.

dipolar moment I_p, magnetic dipolar moment I_m, electric quadrupole dipolar moment I_{EQ}, and magnetic quadrupole dipolar moment I_{MQ}, by using the equations of conventional multipole expansion[68]. As clearly seen in Fig. 4 that, at the broad reflection dip the radiated power I_m is far larger than the radiated power I_{MQ}, and is also several times of I_p and I_{EQ}. This proves that indeed the magnetic dipole contribution is the dominant one.

When a bias voltage is applied to graphene, Fermi energy E_f will be changed, and thus the effective permittivity ε_g of graphene is electrically tunable. Figure 5 presents the dependence of the real and imaginary parts of ε_g on E_f. For each value of E_f, there is a sharp peak of the real part of ε_g in Fig. 5(a), which is related to the narrow interband transition in the monolayer graphene. Correspondingly, the real imaginary part of ε_g exhibits a deep drop for the wavelength to be increased, as clearly seen in Fig. 5(b). Such spectral properties can be easily shifted from 1348 to 1148 nm, when E_f is varied from 0.46 to 0.54 eV.

The narrow interband transition in the monolayer graphene, manifesting itself as a sharp peak of the real part of ε_g in Fig. 5(a), is strongly dependent of Fermi energy E_f. Therefore, the Fano resonance, arising from the coupling between the narrow interband transition and the broad magnetic dipole in metamaterials, can be electrically tuned by applying a bias voltage to graphene to change E_f. To demonstrate this, we have calculated a series of reflection spectra of metamaterials for different E_f. As clearly seen in Fig. 6(a), the position of Fano resonance will red-shift and its asymmetric line shape will become more pronounced, when E_f is continuously decreased to shift the narrow interband transition to be much closer to the broad magnetic dipole. In Fig. 6(b), we have also compared the positions of the interband transition and Fano resonance. Obviously, they are completely overlapped in positions, further confirming that the Fano resonance is indeed the result of the coupling between the interband transition and the magnetic dipole.

We have also studied the effect of the relaxation time of electron-phonon τ on the Fano resonance. In Fig. 7 we present a series of reflection spectra of metamaterials for different τ. When τ is increased from 0.1 to 1.0 ps, the Fano resonance will become more sharp and pronounced. The underlined physics is that, with increasing τ, the imaginary part of the effective permittivity ε_g of graphene is decreased (increased), and thus the light absorption in graphene becomes weak (strong) at the peak (dip) of the Fano resonance.

Finally, we would like to do some discussions on the above numerical results. Naturally occurring materials usually have the saturation of the magnetic response beyond the THz regime. In recent years, exploring artificial metamaterials with various subwavelength building blocks to achieve a strong magnetic response has being drawing a lot of interest. The sharp Fano resonance associated with a magnetic field enhancement may find potential applications in magnetic nonlinearity and magnetic sensing. In a recent work, higher than 60% modulation in the transmission coefficient is reported at near-IR frequencies, by electronically tunable Fano resonance in a hybrid graphene/dielectric metasurface[60]. In our work, the wavelength of the Fano resonance can be conveniently shifted by varying the Fermi energy E_f. The strength of the Fano resonance in the reflection spectra can also be tuned by changing the relaxation time of electron-phonon τ in graphene. As pointed out in ref.[60], such a Fano resonance in the near-IR frequency range would have promising applications, such as biosensing and amplitude modulator.

In conclusion, we have numerically investigated the interesting phenomenon of Fano resonance in metamaterials, consisting of a metal nanodisk array on graphene, a dielectric spacer, and a metal substrate. The near-field plasmon hybridization between individual metal nanodisks and the metal substrate results into the excitation of a broad magnetic dipole. There exists a narrow interband transition dependent of Fermi energy E_f, which manifests itself as a sharp peak of the real part (or an abrupt change of the imaginary part) of the effective permittivity ε_g of graphene. The strong coupling between the narrow interband transition and the broad magnetic dipole leads to the appearance of Fano resonance. The Fano resonance can be electrically tuned by applying a bias voltage to graphene to vary E_f. The position of Fano resonance will be shifted obviously and its asymmetric line shape will become more pronounced, when E_f is varied for the narrow interband transition to progressively approach the broad magnetic dipole.

Method

Simulation. In this work, the reflection and absorption spectra, and the distributions of electromagnetic fields are calculated by "EastFDTD, version 5.0"[61]. In our numerical calculations, two perfectly matching layers (PML) in the z-axis direction are applied to eliminate the boundary scattering, and periodic boundary conditions are used for the x (y)-axis directions. For the graphene monolayer with a thickness of 0.35 nm, the minimum mesh size is set to be 0.05 nm. In the other calculated region, a refined homogeneous mesh size of $\Delta s = 2$ nm and a time step of $\Delta t = \Delta s/2c$ (c is light speed in vacuum) are set manually to ensure numerical convergence. To obtain the reflection and absorption spectra, a Gauss pulse with a center wavelength of 1400 nm is utilized as a light source. The distributions of electromagnetic fields at a plane can be recorded conveniently by using this software package.

References

1. Luk'yanchuk, B. *et al*. The Fano resonance in plasmonic nanostructures and metamaterials. *Nat. Mater.* **9**, 707–715 (2010).
2. Miroshnichenko, A. E., Flach, S. & Kivshar, Y. S. Fano resonances in nanoscale structures. *Rev. Mod. Phys.* **82**, 2257–2298 (2010).
3. Rahmani, M., Luk'yanchuk, B. & Hong, M. H. Fano resonance in novel plasmonic nanostructures. *Laser Photon. Rev.* **7**, 329–349 (2013).
4. Khanikaev, A. B., Wu, C. H. & Shvets, G. Fano-resonant metamaterials and their applications. *Nanophotonics* **2**, 247–264 (2014).
5. Hao, F. *et al*. Symmetry breaking in plasmonic nanocavities: subradiant LSPR sensing and a tunable Fano resonance. *Nano Lett.* **8**, 3983–3988 (2008).
6. Hao, F., Nordlander, P., Sonnefraud, Y., Van Dorpe, P. & Maier, S. A. Tunability of subradiant dipolar and Fano-type plasmon resonances in metallic ring/disk cavities: implications for nanoscale optical sensing. *ACS Nano* **3**, 643–652 (2009).
7. Zhang, S. P., Bao, K., Halas, N. J., Xu, H. X. & Nordlander, P. Substrate-induced Fano resonances of a plasmonic nanocube: a route to increased-sensitivity localized surface plasmon resonance sensors revealed. *Nano Lett.* **11**, 1657–1663 (2011).
8. Wu, C. H. *et al*. Fano-resonant asymmetric metamaterials for ultrasensitive spectroscopy and identification of molecular monolayers. *Nat. Mater.* **11**, 69–75 (2012).
9. Yanik, A. A. *et al*. Seeing protein monolayers with naked eye through plasmonic Fano resonances. *Proc. Natl. Acad. Sci. USA* **108**, 11784–11789 (2011).
10. Lu, H., Liu, X. M., Mao, D. & Wang, G. X. Plasmonic nanosensor based on Fano resonance in waveguide-coupled resonators. *Opt. Lett.* **37**, 3780–3782 (2012).

11. Mass, T. W. W. & Taubner, T. Incident angle-tuning of infrared antenna array resonances for molecular sensing. *ACS Photonics* **2**, 1498–1504 (2015).
12. Zhan, S. P. *et al*. Tunable nanoplasmonic sensor based on the asymmetric degree of Fano resonance in MDM waveguide. *Sci. Rep.* **6**, 22428 (2016).
13. Ye, J. *et al*. Plasmonic nanoclusters: near field properties of the Fano resonance interrogated with SERS. *Nano Lett.* **12**, 1660–1667 (2012).
14. Zhou, Z. K. *et al*. Tuning gold nanorod-nanoparticle hybrids into plasmonic Fano resonance for dramatically enhanced light emission and transmission. *Nano Lett.* **11**, 49–55 (2011).
15. Ridolfo, A., Di Stefano, O., Fina, N., Saija, R. & Savasta, S. Quantum plasmonics with quantum dot-metal nanoparticle molecules: influence of the Fano effect on photon statistics. *Phys. Rev. Lett.* **105**, 263601 (2010).
16. Thyagarajan, K., Butet, J. & Martin, O. J. F. Augmenting second harmonic generation using Fano resonances in plasmonic systems. *Nano Lett.* **13**, 1847–1851 (2013).
17. Zhang, Y., Wen, F. F., Zhen, Y. R., Nordlander, P. & Halas, N. J. Coherent Fano resonances in a plasmonic nanocluster enhance optical four-wave mixing. *Proc. Natl. Acad. Sci. USA* **110**, 9215–9219 (2013).
18. Wu, C. H., Khanikaev, A. B. & Shvets, G. Broadband slow light metamaterial based on a double-continuum Fano resonance. *Phys. Rev. Lett.* **106**, 107403 (2011).
19. Sonnefraud, Y. *et al*. Experimental realization of subradiant, superradiant, and Fano Resonances in ring/disk plasmonic nanocavities. *ACS Nano* **4**, 1664–1670 (2010).
20. Fang, Z. Y. *et al*. Removing a wedge from a metallic nanodisk reveals a Fano resonance. *Nano Lett.* **11**, 4475–4479 (2011).
21. Tang, C. J. *et al*. Localized and delocalized surface-plasmon-mediated light tunneling through monolayer hexagonal-close-packed metallic nanoshells. *Phys. Rev. B* **80**, 165401 (2009).
22. Pena-Rodriguez, O., Rivera, A., Campoy-Quiles, M. & Pal, U. Tunable Fano resonance in symmetric multilayered gold nanoshells. *Nanoscale* **5**, 209–216 (2013).
23. Verellen, N. *et al*. Fano resonances in individual coherent plasmonic nanocavities. *Nano Lett.* **9**, 1663–1667 (2009).
24. Dregely, D., Hentschel, M. & Giessen, H. Excitation and tuning of higher-order Fano resonances in plasmonic oligomer clusters. *ACS Nano* **5**, 8202–8211 (2011).
25. Qi, J. W. *et al*. Independently tunable double Fano resonances in asymmetric MIM waveguide structure. *Opt. Express* **22**, 14688–14695 (2014).
26. Deng, Z. L. *et al*. Full controlling of Fano resonances in metal-slit superlattice. *Sci. Rep.* **5**, 18461 (2015).
27. Cui, Y. H., Zhou, J. H., Tamma, V. A. & Park, W. Dynamic tuning and symmetry lowering of Fano resonance in plasmonic nanostructure. *ACS Nano* **6**, 2385–2393 (2012).
28. Chang, W. S. *et al*. A plasmonic Fano switch. *Nano Lett.* **12**, 4977–4982 (2012).
29. Fedotov, V. A. *et al*. Temperature control of Fano resonances and transmission in superconducting metamaterials. *Opt. Express* **18**, 9015–9019 (2010).
30. Tian, J. B. *et al*. Actively tunable Fano resonances based on colossal magneto-resistant metamaterials. *Opt. Lett.* **40**, 1286–1289 (2015).
31. Zhu, Y., Hu, X. Y., Huang, Y. Y., Yang, H. & Gong, Q. H. Fast and low-power all-optical tunable Fano resonance in plasmonic microstructures. *Adv. Opt. Mater.* **1**, 61–67 (2013).
32. Cao, T., Wei, C. W., Simpson, R. E., Zhang, L. & Cryan, M. J. Fast tuning of double Fano resonance using a phase-change metamaterial under low power intensity. *Sci. Rep.* **4**, 4463 (2014).
33. Hayashi, S. *et al*. Light-tunable Fano resonance in metal-dielectric multilayer structures. *Sci. Rep.* **6**, 33144 (2016).
34. Ferrari, A. C. *et al*. Science and technology roadmap for graphene, related two-dimensional crystals, and hybrid systems. *Nanoscale* **7**, 4598–4810 (2015).
35. Mousavi, S. H. *et al*. Inductive tuning of Fano-resonant metasurfaces using plasmonic response of graphene in the mid-infrared. *Nano Lett.* **13**, 1111–1117 (2013).
36. Emani, N. K. *et al*. Electrical modulation of Fano resonance in plasmonic nanostructures using grapheme. *Nano Lett.* **14**, 78–82 (2014).
37. Dabidian, N. *et al*. Electrical switching of infrared light using graphene integration with plasmonic Fano resonant metasurfaces. *ACS Photonics* **2**, 216–227 (2015).
38. Smirnova, D. A., Miroshnichenko, A. E., Kivshar, Y. S. & Khanikaev, A. B. Tunable nonlinear graphene metasurfaces. *Phys. Rev. B* **92**, 161406 (2015).
39. de Ceglia, D. *et al*. Tuning infrared guided-mode resonances with grapheme. *J. Opt. Soc. Am. B* **33**, 426–433 (2016).
40. Dabidian, N. *et al*. Experimental demonstration of phase modulation and motion sensing using graphene-integrated metasurfaces. *Nano Lett.* **16**, 3607–3615 (2016).
41. Xiao, S. Y. *et al*. Strong interaction between graphene layer and Fano resonance in terahertz metamaterials. *J. Phys. D: Appl. Phys.* **50**, 195101 (2017).
42. Amin, M., Farhat, M. & Bagci, H. A dynamically reconfigurable Fano metamaterial through graphene tuning for switching and sensing applications. *Sci. Rep.* **3**, 2105 (2013).
43. Chen, Z. X. *et al*. Tunable Fano resonance in hybrid graphene-metal gratings. *Appl. Phys. Lett.* **104**, 161114 (2014).
44. Zhang, Y. P. *et al*. A graphene based tunable terahertz sensor with double Fano resonances. *Nanoscale* **7**, 12682–12688 (2015).
45. Ding, J. *et al*. Dynamically tunable Fano metamaterials through the coupling of graphene grating and square closed ring resonator. *Plasmonics* **10**, 1833–1839 (2015).
46. Yang, Y., Zhang, X. F., Huang, A. P. & Xiao, Z. S. Tunable Fano resonant optical forces exerted on a graphene-coated dielectric particle by a Gaussian evanescent wave. *EPL* **116**, 24006 (2016).
47. He, X. Y., Lin, F. T., Liu, F. & Shi, W. Z. Terahertz tunable graphene Fano resonance. *Nanotechnology* **27**, 485202 (2016).
48. Tang, W. W. *et al*. Dynamic metamaterial based on the graphene split ring high-Q Fano-resonnator for sensing applications. *Nanoscale* **8**, 15196–15204 (2016).
49. Guo, J., Jiang, L. Y., Dai, X. Y. & Xiang, Y. J. Tunable Fano resonances of a graphene/waveguide hybrid structure at mid-infrared wavelength. *Opt. Express* **24**, 4740–4748 (2016).
50. Pan, M. Y., Liang, Z. X., Wang, Y. & Chen, Y. H. Tunable angle-independent refractive index sensor based on Fano resonance in integrated metal and graphene nanoribbons. *Sci. Rep.* **6**, 29984 (2016).
51. Yue, J., Shang, X. J., Zhai, X. & Wang, L. L. Numerical investigation of a tunable Fano-like resonance in the hybrid construction between graphene nanorings and graphene grating. *Plasmonics* **12**, 523–528 (2017).
52. Christ, A. *et al*. Controlling the Fano interference in a plasmonic lattice. *Phys. Rev. B* **76**, 201405 (2007).
53. Sheikholeslami, S. N., García-Etxarri, A. & Dionne, J. A. Controlling the interplay of electric and magnetic modes via Fano-like plasmon resonances. *Nano Lett.* **11**, 3927–3934 (2011).
54. Singh, R., Al-Naib, I. A. I., Koch, M. & Zhang, W. L. Sharp Fano resonances in THz metamaterials. *Opt. Express* **19**, 6312–6319 (2011).
55. Cao, W. *et al*. Low-loss ultra-high-Q dark mode plasmonic Fano metamaterials. *Opt. Lett.* **37**, 3366–3368 (2012).
56. Miroshnichenko, A. E. & Kivshar, Y. S. Fano Resonances in all-dielectric oligomers. *Nano Lett.* **12**, 6459–6463 (2012).

57. Shafiei, F. *et al*. A subwavelength plasmonic metamolecule exhibiting magnetic-based optical Fano resonance. *Nat. Nanotechnol.* **8**, 95–99 (2013).
58. Nazir, A. *et al*. Fano coil-type resonance for magnetic hot-spot generation. *Nano Lett.* **14**, 3166–3171 (2014).
59. Panaro, S. *et al*. Plasmonic moon: a Fano-like approach for squeezing the magnetic field in the infrared. *Nano Lett.* **15**, 6128–6134 (2015).
60. Argyropoulos, C. Enhanced transmission modulation based on dielectric metasurfaces loaded with graphene. *Opt. Express* **23**, 23787–23797 (2015).
61. Website: www.eastfdtd.com.
62. Johnson, P. B. & Christy, R. W. Optical constants of the noble metals. *Phys. Rev. B* **6**, 4370–4379 (1972).
63. Zhu, B. F., Ren, G. B., Zheng, S. W., Lin, Z. & Jian, S. S. Nanoscale dielectric-graphene-dielectric tunable infrared waveguide with ultrahigh refractive indices. *Opt. Express* **21**, 17089–17096 (2013).
64. Xiang, Y. J., Guo, J., Dai, X. Y., Wen, S. C. & Tang, D. Y. Engineered surface Bloch waves in graphene-based hyperbolic metamaterials. *Opt. Express* **22**, 3054–3062 (2014).
65. Hao, J. *et al*. High performance optical absorber based on a plasmonic metamaterial. *Appl. Phys. Lett.* **96**, 251104 (2010).
66. Song, Z. Y. & Zhang, B. L. Wide-angle polarization-insensitive transparency of a continuous opaque metal film for nearinfrared light. *Opt. Express* **22**, 6519–6525 (2014).
67. Tang, C. J. *et al*. Ultrathin amorphous silicon thin-film solar cells by magnetic plasmonic metamaterial absorbers. *RSC Adv.* **5**, 81866–81874 (2015).
68. Papasimakis, N., Fedotov, V. A., Savinov, V., Raybould, T. A. & Zheludev, N. I. Electromagnetic toroidal excitations in matter and free space. *Nat. Mater.* **15**, 263–271 (2016).

Acknowledgements

This work is financially supported by the NSFC under Grant Nos. 11304159 and 11104136, the NSFZJ under Grant No. LY14A040004, the Natural Science Foundation of Jiangsu Province (NSFJS) under Grant No. BK20161512, the Qing Lan Project of Jiangsu Province, the Open Project of State Key Laboratory of Millimeter Waves under Grant No. K201821, and the NUPTSF under Grant No. NY217045.

Author Contributions

Bo Liu, Chaojun Tang and Jing Chen did the calculations. Chaojun Tang and Jing Chen wrote the manuscript. Chaojun Tang and Jing Chen supervised the project. Bo Liu, Chaojun Tang, Jing Chen, Mingwei Zhu, Mingxu Pei, and Xiaoqin Zhu discussed the results and reviewed the manuscript.

Additional Information

Competing Interests: The authors declare that they have no competing interests.

Publisher's note: Springer Nature remains neutral with regard to jurisdictional claims in published maps and institutional affiliations.